Heliyon 7 (2021) e07112

Contents lists available at ScienceDirect

Heliyon

journal homepage: www.cell.com/heliyon

Research article

Remarkable vessel enlargement within lung consolidation in COVID-19 compared to AH1N1 pneumonia: A retrospective study in Italy

Andrea Bianco [a,b], Tullio Valente [c], Fabio Perrotta [d], Elvira Stellato [e,*], Luca Brunese [d], Brad J. Wood [f], Gianpaolo Carrafiello [g,h], Roberto Parrella [i], Study Investigators

[a] Department of Translational Medical and Surgical Science, University of Campania Luigi Vanvitelli, Naples, Italy
[b] COViD Unit PNL Vanvitelli, Hospital Monaldi, A.O. R.N. dei Colli, Naples, Il Italy
[c] Department of Radiology, Monaldi Hospital, A.O.R.N. dei Colli, Naples, Italy
[d] Department of Medicine and Health Sciences "V. Tiberio", University of Molise, Campobasso, Italy
[e] Postgraduate School of Diagnostic and Interventional Radiology, University of Milan, Milan, Italy
[f] Center for Interventional Oncology, Radiology and Imaging Science, National Institutes of Health, Bethesda, USA
[g] Radiology Department, Foundation IRCCS Ca' Granda Ospedale Maggiore Policlinico, Milan, Italy
[h] Department of Health Sciences, Università degli Studi di Milano, Milan, Italy
[i] Department of Infectious Diseases, COVID Unit D. Cotugno Hospital, A.O.R.N. dei Colli, Naples, Italy

ARTICLE INFO

Keywords:
COVID-19
SARS-CoV-2
AH1N1 influenza
Chest computed tomography
Vascular enlargement

ABSTRACT

Purpose: To investigate the early CT findings in COVID-19 pneumonia as compared to influenza A virus H1N1 (AH1N1), with focus on vascular enlargement within consolidation or ground glass opacity (GGO) areas.
Methods: 50 patients with COVID-19 pneumonia were retrospectively compared to 50 patients with AH1N1 pneumonia diagnosed during the 2009 pandemic. Two radiologists reviewed chest CT scans independently and blindly, with discordance resolved by consensus. Dilated or tortuous vessels within hyperdense lesions were recorded.
Results: COVID-19 pneumonia presented with bilateral (96%), peripheral areas of GGO (22%), consolidation (4%) or combined GGO-consolidation (74%). The vascular enlargement sign in COVID-19 pneumonia was much more commonly present in COVID-19 (45/50, 90%) versus AH1N1 pneumonia (12/50, 24%) ($p < 0.001$). Vascular enlargement was more often present in lower lobes with a peripheral distribution.
Conclusions: Vascular enlargement in consolidative/GGO areas may represent a reasonably common early CT marker in COVID-19 patients and is of uncertain etiology. Although speculative, theoretical mechanisms could potentially reflect acute inflammatory changes, pulmonary endothelial activation, or acute stasis. Further studies are necessary to verify specificity and to study if prognostic for clinical outcomes.

Summary at Glance

Vascular enlargement within consolidations and ground glass opacities are highly present among hospitalized COVID-19 patients as compared with AH1N1 pneumonia. These data may suggest vascular mechanisms such as microvascular endothelial pathology in COVID-19 pneumonia.

1. Introduction

Severe acute respiratory syndrome coronavirus 2 (SARS-CoV-2) is now spreading globally causing clusters of acute severe respiratory illness and death. The rapid expansion of SARS-CoV-2 since December 2019 from Wuhan China led the World Health Organization (WHO) on March 11 to declare COVID-19 a pandemic. Severe lower respiratory infection was also the major hallmark of the most recent pandemic influenza A

* Corresponding author.
E-mail addresses: elvira.stellato@unimi.it, elvira.stellato@gmail.com (E. Stellato).

https://doi.org/10.1016/j.heliyon.2021.e07112
Received 21 July 2020; Received in revised form 12 December 2020; Accepted 17 May 2021

virus (AH1N1), in 2009 [1]. Both SARS-CoV-2 and AH1N1 viruses retain the critical ability to reach lower airways and enter epithelial cells. Clinical manifestations of both viral diseases range from asymptomatic infection, mild upper respiratory illness, viral syndromes, and severe pneumonia to acute respiratory distress syndrome (ARDS) and progression to multiorgan failure and death. Severe COVID-19 is frequently complicated with dysregulated coagulative homeostasis and deep vein thrombosis (DVT) and pulmonary embolism (PE) are common complications [2, 3, 4].

Chest imaging plays a relevant role in the diagnosis and management of viral infections, especially pneumonia [5, 6]. Although somewhat controversial, it has been reported that chest CT has higher sensitivity for the diagnosis of COVID-19 than some initial reverse-transcription polymerase chain reaction (RT-PCR) tests, and may be considered as a primary targeted focused tool for COVID-19 diagnosis in high prevalence outbreak locations [7]. Identifying chest CT scan features in viral pneumonia might lead to a better understanding of the pathophysiological changes occurring in infection, which in turn could inform decisions regarding therapy [5]. Chest CT scan characteristics during AH1N1 infection have been characterized, and features of SARS-CoV-2 infection have been progressively identified during the ongoing pandemic. Data comparing radiological features of AH1N1 influenza and COVID-19 may further contribute to understanding pathophysiological features of SARS Cov2 infection.

2. Materials and methods

2.1. Study population

A retrospective single-center study was approved by the local Ethics Committee and conducted according to the ethical principles of the Declaration of Helsinki. Written informed consent was waived by the Ethics Committee. Fifty consecutive patients with a diagnosis of SARS-CoV-2 confirmed by laboratory-based RT-PCR were admitted to the hospital for respiratory symptoms [8, 9]; this study population was compared to AH1N1 influenza patient cohort of equal number diagnosed during the 2009 pandemic [10] at the same institution. The study group 1 consisted of 50 COVID-19 patients admitted to a COVID unit (38 treated in the respiratory unit and 12 admitted to ICU); study group 2 included 50 AH1N1 patients (balanced as 38 admitted to the respiratory unit and 12 to the ICU) from medical records. All patients underwent baseline HRCT scanning with the following two scanners: a 16-MDCT Brilliance scanner (Philips Healthcare) in AH1N1 2009 pneumonia cohort, and a 64-MDCT LightSpeed VCT (GE Healthcare) in COVID-19 pneumonia cohort. The acquisition parameters were set at 120 kVp; 100–200 mAs; pitch, 0.75–1.5; and collimation 1-1,25 mm. All imaging data were reconstructed using a high sharp reconstruction algorithm with a slice thickness of 1–1.5 mm. Baseline CT images were, when feasible, acquired at full inspiration with the patient in the supine position without any positive respiratory support (end-expiratory positive pressure and/or pressure support).

2.2. Image assessment

Two radiologists (13 and 20 years of experience) reviewed chest CT scans blindly and independently, by consensus. All images were viewed with both lung (width, 1500 HU; level, −700 HU) and mediastinal (width, 350 HU; level, 40 HU) settings. 16 imaging features were recorded: ground-glass opacities (GGO), consolidation, mixed GGO and consolidation, air bronchogram sign, centrilobular nodules and tree-in-bud, architectural distortion, cavitation, bronchial wall thickening and airways secretions, reticulation and linear opacities, crazy-paving pattern, subpleural bands, traction bronchiectasis, “reverse halo” sign, subpleural transparent line, intrathoracic lymph node enlargement, and pleural thickening or retraction or effusions [3, 11, 12, 13, 14, 15, 16]. The focus was placed on the presence and distribution of “vascular enlargement in the hyperdense (GGO and/or consolidation) lesion” on HRCT [15]. The “vascular enlargement in the hyperdense lesion” finding has been postulated to represent dilated or tortuous vessels seen within hyperdense lesions, probably caused by an acute inflammatory response and/or intussusceptive angiogenesis [17, 18, 19].

2.3. Statistical analysis

Continuous variables were expressed as mean (±standard deviation) or median (IQR) whether non-normal distribution. Categorical variables were expressed as number (%) and compared by χ^2 test or Fisher's exact test between AH1N1 and COVID-19 groups. Multivariate regression models were used to determine the independent risk factors for death during hospitalization. Statistical analyses were done using the SPSS (v 23.0) Software Package (SPSS, Inc., Chicago, IL, USA). A two-sided α of less than 0.05 was considered statistically significant.

3. Results

The study population characteristics and radiologic findings of AH1N1 and COVID-19 patients are listed in Table 1. The COVID-19 patient cohort had a higher percentage of men than in AH1N1 group (35/50 [70%] versus 22/50 [44%]; $p = 0.01$). The most common AH1N1 pneumonia HRCT findings were ground-glass opacities (14/50 [28%]), consolidations (6/50 [12%]), a combination of ground-glass opacities and consolidations (30/50 [60%]). Other HRCT features were airspace nodules (2/50 [4%]), bronchial wall thickening (2/50 [4%]), interlobular septal thickening (3/50 [6%]), crazy-paving pattern (6/50 [12%]), peri-lobular pattern (2/50 [4%]). Pleural effusion in AH1N1 group was present in 14/50 (28%) of patients versus 3/50 (6%) of COVID-19 patients ($p = 0.003$). On the other hand, the hallmarks of COVID-19 infection at baseline HRCT imaging were bilateral (48/50 [96%]), peripheral areas of ground-glass (11/50 [22%]), consolidation (2/50 [4%]) or combined GGO-consolidation (37/50 [74%]). GGOs presented as rounded morphology and often with a peripheral lung distribution (Figure 1). COVID-19 pneumonia often showed as bilateral multi-lobar GGOs mainly involving the lower lobes (85%) and less frequently within the right middle lobe (50%) and upper lobes (66%). Crazy-paving pattern was present in 4/50 (8%) of patients. Tree-in-bud pattern, pleural effusions, hilar and mediastinal lymphadenopathy have been uncommon. A vascular enlargement in the hyperdense lesion (Figure 2) was commonly found in 45/50 [90%] of COVID-19 patients, while it was retrospectively present only in 12/50 [24%] $p < 0.001$ of AH1N1 patients. In COVID-19 pneumonia this HRCT sign was more likely to have a peripheral distribution (88%) and bilateral involvement (83%) and be lower lung predominant (63%) and multifocal (68%). Interestingly, vascular enlargement in hyperdense areas was present in 8/8 (100%) of COVID-19 patients with severe respiratory failure admitted to ICU. Laboratory findings of COVID-19 patients according to the presence of vascular enlargement are presented in Table 2. Finally, we found subpleural bands in 9/50 (18%) COVID-19 patients while no AH1N1 patients documented this sign ($p = 0.002$). In the COVID-19 group, 9/50 patients (18%) died during hospitalization whereas 4/50 (8%) AH1N1 died. Multivariate analysis found no independent risk factor for mortality (Table 3).

4. Discussion

CT is considered the routine imaging modality for diagnosis and monitoring patients with clinically severe viral pneumonia. Radiological presentation is highly heterogenous and potentially evolutive. While GGOs, consolidations, vascular enlargement, crazy paving, interlobular septal thickening and air bronchogram reflect typical COVID-19 presentation, uncommon signs (bronchiectasis, lymphadenopathy, halo sign, reverse halo sign, pleural or pericardial effusion and cavitation) could be present though their clinical significance remains unclear [20].

Table 1. Clinical characteristics and radiological findings in the study population.

	All patients (n.100) n.(%)	H1N1 patients (n. 50) n.(%)	COVID-19 patients (n.50) n.(%)	p
Sex				**0.008**
Male	57 (57%)	22 (44%)	35 (70%)	
Female	43 (43%)	28 (56%)	15 (30%)	
Age (yrs.) mean ± DS	49.4 ± 13.8	40.90 ± 13.01	57.9 ± 14.6	
Admitted to ICU		8 (16.0%)	8 (16%)	1.00
Imaging findings				
Ground-glass opacities (GGO)	25/100 (25%)	14/50 (28%)	11/50 (22%)	0.49
Consolidations	8/100 (8%)	6/50 (12%)	2/50 (4%)	0.14
Combination of GGO and consolidations	67/100 (67%)	30/50 (60%)	37/50 (74%)	0.13
Airspace nodules	2/100 (2%)	2/50 (4%)	0/50 (0%)	0.15
Tree-in-bud	2/100 (2%)	2/50 (4%)	0/50 (0%)	0.15
Septal lines	7/100 (7%)	3/50 (6%)	4/50 (8%)	0.69
Crazy-paving pattern	10/100 (10%)	6/50 (12%)	4/50 (8%)	0.50
Perilobular pattern	2/100 (2%)	2/50 (4%)	0/50 (0%)	0.15
Subpleural bands	9/100 (9%)	0/50 (0%)	9/50 (18%)	**0.002**
Intrathoracic lymph node enlargement	8/100 (8%)	6/50 (12%)	2/50 (4%)	0.14
Vascular enlargement	57/100 (57%)	12/50 (24%)	45/50 (90%)	**< 0.001**
Pleural effusion	17/100 (17%)	14/50 (28%)	3/50 (6%)	**0.003**
Pneumothorax	1/100 (1%)	0 (0%)	1 (2%)	0.31
Reverse "Halo"	6/100 (6%)	3/50 (6%)	3/50 (6%)	1
Lung predominance				**0.01**
Upper lung predominant	15/100 (15%)	12/50 (24%)	3/50 (6%)	
Lower lung predominant	82/100 (82%)	35/50 (70%)	47/50 (94%)	
No predominance	3/100 (3%)	3/50 (6%)	0 (0%)	
Lung region distribution				**0.02**
Unilateral	11/100 (11%)	9/50 (18%)	2/50 (4%)	
Bilateral	89/100 (89%)	41/50 (82%)	48/50 (96%)	

Data are presented as mean values ± Standard Deviation or absolute number (percentage). Statistically significant values in bold. GGO: Ground-Glass Opacity; ICU: Intensive Care Unit.

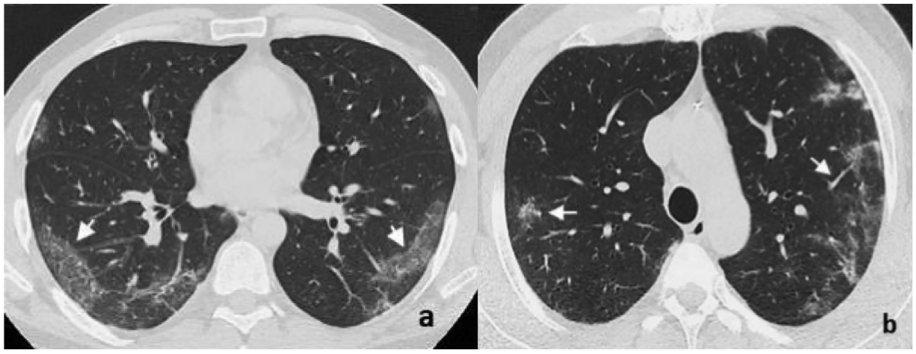

Figure 1. a. HRCT in a COVID-19 pneumonia patient shows bilateral patchy multilobar GGOs with peripheral posterior distribution, mainly in the lower lobes (*arrows*). b. A 58-year-old man with fever (38.3 °C), cough, dyspnea and laboratory-confirmed COVID-19 pneumonia; HRCT shows bilateral involvement with peripheral rounded GG opacities and vascular enlargement in GGO lesions (*arrows*).

In the present study, we investigated about the main radiological CT differences between patients with COVID-19 and patients with AH1N1 diagnosed during the 2009 pandemic. We found that peripheral and peribronchovascular GGO/consolidations distribution was common both in patients with COVID-19 pneumonia as well in patients with influenza AH1N1 pneumonia. Interestingly, we showed that subpleural fibrotic stripes, vascular enlargement or thickening within hyperdense lesions, and bilateral lower lungs predominance might guide the differential diagnosis. A significantly higher prevalence of vascular enlargement within the GGO or consolidative pattern in COVID-19 patients was present compared to patients with AH1N1 pneumonia (45/50 [90%] versus 12/50 [24%], $p < 0.001$). The increased diameter of the vascular segment with tortuous flow within a lesion area in COVID-19 patients might represent acute changes in inflammatory host response [18], endothelial upregulation of inflammation, or perhaps stasis. Our results support recent advances illustrated in COVID-19 literature. Patel et al. in an observational study documented dilated pulmonary vessels in 21/33 (63.6%) of mechanically ventilated COVID-19 patients; in particular in 10/21 patients (47.6%), this finding was present also in absence of pulmonary embolism [21]. In another radiological study, subsegmentary vessel enlargement within areas of inflammation was described as a typical feature among COVID-19 patients (89%). Though limited by the small number of patients, vascular enlargement was present in all the patients with mild disease [22]. However, the complex network

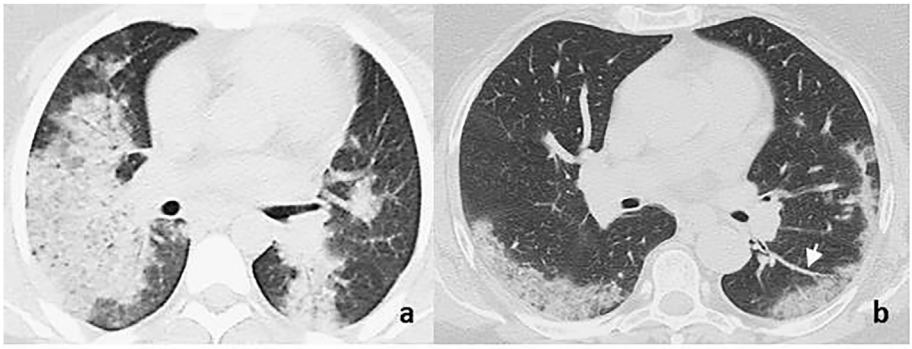

Figure 2. H1N1 *vs* COVID-19" Vascular enlargement": HRCT finding. a) A 31-year-old man with fatty liver, alteration of functional liver indices and drug abuse in H1N1 pneumonia. Clinical findings: fever (38.2 °C), jaundice, acute respiratory failure. Axial MDCT scans at lung middle zones show bilateral involvement with rounded multifocal peripheral GGOs confluent in central consolidation and air bronchogram; no vascular enlargement is visible. b) A 60-year-old woman with fever (38.5 °C), non-productive cough and lymphopenia in laboratory-confirmed COVID-19 pneumonia. Axial HRCT shows bilateral lower lobes subpleural GGOs and vascular enlargement on the left base (*arrow*).

Table 2. Laboratory findings and CT Severity Score in COVID-19 patients.

	COVID-19 (n.50)	Vascular Enlargement - (n. 5)	Vascular Enlargement + (n. 45)
WBC (x103/uL)	7.0 ± 3.54	11.0 ± 5.6	6.6 ± 3.1
Neutrophils (x103/uL)	5.615 ± 3.52	9.235 ± 5.73	5.253 ± 3.12
Lymphocytes (x103/uL)	0.885 ± 0.37	1.123 ± 0.60	0.862 ± 0.34
Monocytes (x103/uL)	0.462 ± .25	0.430 ± 0.22	0.465 ± 0.26
Eosinophils (x103/uL)	0.013 ± 0.03	0.02 ± 0.01	0.013 ± 0.03
RBC (x106/uL)	4.768 ± 0.53	4.773 ± 0.56	4.768 ± 0.53
Hb (g/dl)	13.9 ± 1.64	14.1 ± 1.1	13.9 ± 1.7
HTC %	40.1 ± 4.38	40.3 ± 4.6	40.1 ± 4.4
Platelets (103/uL)	211.3 ± 73.0	268.8 ± 74.2	205.6 ± 71.3
ERS	50.8 ± 23.3	60.0 ± 4.2	49.6 ± 24.6
CPR (mg/dL)	11.3 ± 8.3	19.0 ± 13.2	10.5 ± 7.4
Procalcitonin	0.7 ± 2.7	0.3 ± 0.4	0.7 ± 2.9
IL 2R (IU)	1259.5 ± 611.4	1877.5 ± 355.7	1197.8 ± 601.9
IL-6 (pg/mL)	210.8 ± 439.9	157.7 ± 209.6	216.7 ± 460.5
AST	52.1 ± 27.2	64.5 ± 29.8	50.9 ± 27.0
ALT	52.8 ± 76.6	36.0 ± 21.8	54.4 ± 80.0
LDH (U/L)	402.9 ± 187.2	606.3 ± 312.0	380.9 ± 160.5
Albumin (%)	49.6 ± 5.5	43.8 ± 4.1	50.4 ± 5.3
Albumin/Globulin Ratio	1.0 ± 0.2	0.8 ± 0.1	1.0 ± 0.2
2019-nCoV IgM	3.1 ± 4.6	1.6 ± 1.7	3.2 ± 4.8
2019-nCoV IgG	40.2 ± 30.8	26.6 ± 37.3	41.4 ± 30.8
CT Severity Score	9.63 ± 4.1	13.2 ± 7.6	9.3 ± 3.6
Death n. (%)	9/50 (18)	1/5 (20)	4/45 (8.9)

Data are presented as mean values ± Standard Deviation.

underlying SARS-CoV2 vascular trophism, enhanced inflammation and the clinical consequences of hypercoagulative status are still not fully clarified. In fact, COVID-19 spectrum of disease is heterogeneous and severity of evolution is variable. Gattinoni et al. described two different COVID-19 ARDS phenotypes. In the early COVID-19 phase (type 1 or L-phenotype) respiratory system compliance and weight are preserved, there is low response to PEEP and respiratory failure is mainly sustained by altered V/Q ratio. In this group of patients, dual energy CT reveals a combination of hyperperfused GGO or consolidative areas with reduced iodine distribution within preserved lung parenchyma. Subsequently, in advanced stages (type 2 or H-phenotype) a classical ARDS model can develop (high elastance, high right-to-left shunt caused by elevated perfusion in non-aerated tissue and higher lung recruitability) [23, 24].

Subsequently, our findings confirm that COVID-19 vascular involvement is widely present in early phase of pneumonia, while in other viral pneumonia might not be present. Clinical and radiological differences between COVID-19 and AH1N1 pneumonia have been investigated in recent studies. Data from a retrospective cohort study in patients with ARDS with COVID-19 or AH1N1 pneumonia showed that despite patients with COVID-19 having a lower SOFA-score, less consolidation areas and higher PaO2/FiO2 ratio at baseline, in-hospital mortality between the two groups was similar [25]. In another small series, Yin et al found that linear opacification, vascular enlargement and crazy paving pattern were radiological signs more frequent in patients with COVID-19 pneumonia than in AH1N1.

Complex molecular mechanisms underlying vascular activation in the early phase of disease have been described. Firstly, the state of acute inflammation could reflect the negative regulation that SARS-CoV2 has on its receptor Angiotensin converting enzyme 2 (ACE2) [26, 27, 28]. ACE2 downregulation is known to be followed by a rise in the level of Angiotensin II (AngII), an overactivation of its receptor AT1R, and transcription of pro-inflammatory cytokines [29, 30]. Release of pro-inflammatory mediators prompted by ACE2 deregulation could be modulated from other metabolic factors including adipose tissue. In a recent research, Watanabe et al. found that interstitial pneumonia radiological severity as evaluated by lung severity score (LSS) was associated with visceral adipose fat [31]. Furthermore, both these factors resulted independently associated with the need of intensive care.

Table 3. Predictors of mortality in n.50 COVID-19 patients.

	Univariate p value	Multivariate p value °
Age	0.32	
WBC (x103/uL)	0.049	0.98
Neutrophils (x103/uL)	0.04	0.95
Lymphocytes (x103/uL)	0.71	
Monocytes (x103/uL)	0.95	
Eosinophils (x103/uL)	0.40	
RBC (x106/uL)	0.93	
Hb (g/dl)	0.46	
HTC %	0.58	
PLT (103/uL)	0.44	
ERS	0.34	
CRP (mg/dL)	0.04	0.47
Procalcitonin	0.76	
IL-2R (IU)	0.10	
IL-6 (pg/mL)	0.21	
AST	0.36	
ALT	0.67	
LDH (U/L)	0.04	0.92
CT Score Severity	0.01	0.26

° Multi-variable model generated using forward selection and backward elimination processes, assessing all variables with a p-value$<$0.05 on univariate analysis.

By contrast AH1N1 uses hemagglutinin glycoproteins to bind specific sialic acids residues linked to glycans present on the surface of the lung alveolar epithelial cells. The impact of these virus/target cell interactions in terms of pathophysiological and radiological findings is not defined [23, 24, 25]. In this scenario, the endothelial activation following viral infection resulting in thrombotic microangiopathy (TMA) should be considered, although it requires further investigation. TMA includes a spectrum of phenotypically analogous diseases driven by intravascular hemolytic anemia and thrombocytopenia and local tissue damage [28]. Furthermore, in ARDS patients with AH1N1 influenza platelet-monocyte aggregates were found more commonly than in patients with ARDS sustained from bacteria pneumonia [31]. In severe respiratory failure, pulmonary vascular impairment can be triggered via the hypoxia-inducible transcription factor-dependent signaling pathway [32].

Altogether the above-mentioned data may offer relevant therapeutic implications in COVID-19 patients. Initial data from a retrospective study reported that COVID-19 patients – who have SIC score $\geq$4 or D-dimer $>$ 6 fold of upper normal limit – treated with anticoagulant (over standard therapy) resulted in lower 28-day mortality [33, 34]. Therefore, the major prevalence of vascular enlargement in COVID-19 patients that we have reported could potentially represent the radiological manifestation of underlying vascular endothelial thrombotic activation, pre-thrombotic inflammation and stress responses, and/or stasis. The data presented here are usually unenhanced, without iodinated contrast, which complicates the assessment for peripheral pulmonary embolism. Secondly, we include both ICU and non-ICU patients that may potentially present different CT phenotypes; further studies in both definite settings would be appropriate. Statistical tests and p values should also be interpreted with caution given the limited number of patients included. Finally, longitudinal studies for tracking the evolution of these changes and appropriate correlation with clinical outcomes are needed.

5. Conclusions

In the present study, we identified relevant chest CT features that may reflect differences in clinical pathways and evolution between AH1N1 and COVID-19 pneumonia. Furthermore, vascular enlargement was uncommon in AH1N1 pneumonia and may help distinguish COVID-19 from AH1N1 pneumonia and other community-acquired pneumonia. Vascular enlargement conveys both diagnostic and prognostic information and may significantly contribute to diagnostic work-up and patient management. Much research is required to define with accuracy the pathophysiological significance and clinical relevance of this radiological occurrence and whether such findings could influence treatment decisions. It remains to be understood whether and to what extent the major SARS-CoV-2 receptor ACE2 and its pathway affects this process. Further studies are urgently required to explore the underlying mechanisms responsible for the vascular enlargement seen on Chest CT.

Declarations

Author contribution statement

Andrea Bianco: Conceived and designed the experiments; Analyzed and interpreted the data; Wrote the paper.

Tullio Valente and Fabio Perrotta: Conceived and designed the experiments; Contributed reagents, materials, analysis tools or data; Wrote the paper.

Roberto Parrella: Conceived and designed the experiments; Wrote the paper.

Luca Brunese and Gianpaolo Carrafiello: Analyzed and interpreted the data.

Elvira Stellato and Brad J. Wood: Analyzed and interpreted the data; Wrote the paper.

Funding statement

This research did not receive any specific grant from funding agencies in the public, commercial, or not-for-profit sectors.

Data availability statement

Data will be made available on request.

Declaration of interests statement

The authors declare no conflict of interest.

Additional information

No additional information is available for this paper.

Acknowledgements

Work supported in part by the NIH Center for Interventional Oncology and the Intramural Research Program of the NIH.

References

[1] R. Perez-Padilla, D. de la Rosa-Zamboni, S. Ponce de Leon, M. Hernandez, F. Quiñones-Falconi, E. Bautista, A. Ramirez-Venegas, J. Rojas-Serrano, C.E. Ormsby, A. Corrales, et al., Pneumonia and respiratory failure from swine-origin influenza A (H1N1) in Mexico, N. Engl. J. Med. 361 (2009) 680–689.

[2] C. Huang, Y. Wang, X. Li, L. Ren, J. Zhao, Y. Hu, L. Zhang, G. Fan, J. Xu, X. Gu, et al., Clinical features of patients infected with 2019 novel coronavirus in Wuhan, China, Lancet 395 (2020) 497–506.

[3] Z. Cheng, Y. Lu, Q. Cao, L. Qin, Z. Pan, F. Yan, W. Yang, Clinical features and chest CT manifestations of coronavirus disease 2019 (COVID-19) in a single-center study in Shanghai, China, AJR Am. J. Roentgenol. 1–6 (2020).

[4] M. Boccia, L. Aronne, B. Celia, G. Mazzeo, M. Ceparano, V.D. Agnano, R. Parrella, T. Valente, A. Bianco, F. Perrotta, COVID-19 and coagulative axis: review of emerging aspects in a novel disease, Monaldi Arch. Chest Dis. 90 (2) (2020 May 19).

[5] H.J. Koo, S. Lim, J. Choe, S.-H. Choi, H. Sung, K.-H. Do, Radiographic and CT features of viral pneumonia, Radiogr. Rev. Publ. Radiol. Soc. North Am. Inc 38 (2018) 719–739.

[6] L. Rinaldi, S. Milione, M.C. Fascione, P.C. Pafundi, C. Altruda, M. Di Caterino, L. Monaco, A. Reginelli, F. Perrotta, G. Porta, et al., Relevance of lung ultrasound in the diagnostic algorithm of respiratory diseases in a real-life setting: a multicentre prospective study, Respirology (2019).
[7] E.Y.P. Lee, M.-Y. Ng, P.-L. Khong, COVID-19 pneumonia: what has CT taught us? Lancet Infect. Dis. 20 (2020) 384–385.
[8] World Health Organization, Clinical Management of Severe Acute Respiratory Infection (SARI) when COVID-19 Disease Is Suspected, 2020, pp. 1–21.
[9] European Centre for Disease Prevention and Control Infection prevention and control for the care of patients with 2019-nCoV in healthcare settings Target audience Healthcare settings 20200202, Elsevier's nov, Coronavirus Inf. Cent. (2020) 3–6.
[10] T. Valente, F. Lassandro, M. Marino, F. Squillante, M. Aliperta, R. Muto, H1N1 pneumonia: our experience in 50 patients with a severe clinical course of novel swine-origin influenza A (H1N1) virus (S-OIV), Radiol. Med. 117 (2012) 165–184.
[11] Y. Li, L. Xia, Coronavirus disease 2019 (COVID-19): role of chest CT in diagnosis and management, AJR Am. J. Roentgenol. 1–7 (2020).
[12] R. Han, L. Huang, H. Jiang, J. Dong, H. Peng, D. Zhang, Early clinical and CT manifestations of coronavirus disease 2019 (COVID-19) pneumonia, AJR Am. J. Roentgenol. (2020) 1–6.
[13] J. Lei, J. Li, X. Li, X. Qi, CT imaging of the 2019 novel coronavirus (2019-nCoV) pneumonia, Radiology 295 (2020) 18.
[14] M. Chung, A. Bernheim, X. Mei, N. Zhang, M. Huang, X. Zeng, J. Cui, W. Xu, Y. Yang, Z.A. Fayad, et al., CT imaging features of 2019 novel coronavirus (2019-nCoV), Radiology 295 (2020) 202–207.
[15] A. Bernheim, X. Mei, M. Huang, Y. Yang, Z.A. Fayad, N. Zhang, K. Diao, B. Lin, X. Zhu, K. Li, et al., Chest CT findings in coronavirus disease-19 (COVID-19): relationship to duration of infection, Radiology (2020) 200463.
[16] S. Salehi, A. Abedi, S. Balakrishnan, A. Gholamrezanezhad, Coronavirus disease 2019 (COVID-19): a systematic review of imaging findings in 919 patients, AJR Am. J. Roentgenol. (2020) 1–7.
[17] X. Xie, Z. Zhong, W. Zhao, C. Zheng, F. Wang, J. Liu, Chest CT for typical 2019-nCoV pneumonia: relationship to negative RT-PCR testing, Radiology (2020) 200343.
[18] F. Gao, M. Li, X. Ge, X. Zheng, Q. Ren, Y. Chen, F. Lv, Y. Hua, Multi-detector spiral CT study of the relationships between pulmonary ground-glass nodules and blood vessels, Eur. Radiol. 23 (2013) 3271–3277.
[19] M. Ackermann, S.E. Verleden, M. Kuehnel, A. Haverich, T. Welte, F. Laenger, A. Vanstapel, C. Werlein, H. Stark, A. Tzankov, et al., Pulmonary vascular endothelialitis, thrombosis, and angiogenesis in covid-19, N. Engl. J. Med. 383 (2020) 120–128.
[20] D. Caruso, T. Polidori, G. Guido, M. Nicolai, B. Bracci, A. Cremona, M. Zerunian, M. Polici, F. Pucciarelli, C. Rucci, et al., Typical and atypical COVID-19 computed tomography findings, World J. Clin. Cases 8 (2020) 3177–3187.
[21] B.V. Patel, D.J. Arachchillage, C.A. Ridge, P. Bianchi, J.F. Doyle, B. Garfield, S. Ledot, C. Morgan, M. Passariello, S. Price, et al., Pulmonary angiopathy in severe COVID-19: physiologic, imaging, and hematologic observations, Am. J. Respir. Crit. Care Med. 202 (2020) 690–699.
[22] D. Caruso, M. Zerunian, M. Polici, F. Pucciarelli, T. Polidori, C. Rucci, G. Guido, B. Bracci, C. De Dominicis, A. Laghi, Chest CT features of COVID-19 in rome, Italy, Radiology 296 (2020) E79–E85.
[23] M. Lang, A. Som, D.P. Mendoza, E.J. Flores, N. Reid, D. Carey, M.D. Li, A. Witkin, J.M. Rodriguez-Lopez, J.-A.O. Shepard, et al., Hypoxaemia related to COVID-19: vascular and perfusion abnormalities on dual-energy CT, Lancet Infect. Dis. 20 (2020) 1365–1366.
[24] M.G. Santamarina, D. Boisier, R. Contreras, M. Baque, M. Volpacchio, I. Beddings, COVID-19: a hypothesis regarding the ventilation-perfusion mismatch, Crit. Care 24 (2020) 4–7.
[25] X. Tang, R.H. Du, R. Wang, T.Z. Cao, L.L. Guan, C.Q. Yang, Q. Zhu, M. Hu, X.Y. Li, Y. Li, et al., Comparison of hospitalized patients with ARDS caused by COVID-19 and H1N1, Chest 158 (2020) 195–205.
[26] I. Glowacka, S. Bertram, P. Herzog, S. Pfefferle, I. Steffen, M.O. Muench, G. Simmons, H. Hofmann, T. Kuri, F. Weber, et al., Differential downregulation of ACE2 by the spike proteins of severe acute respiratory syndrome coronavirus and human coronavirus NL63, J. Virol. 84 (2010) 1198–1205.
[27] F. Perrotta, M.G. Matera, M. Cazzola, A. Bianco, Severe respiratory SARS-CoV2 infection: does ACE2 receptor matter? Respir. Med. 168 (2020) 105996.
[28] F. Scialo, A. Daniele, F. Amato, L. Pastore, M.G. Matera, M. Cazzola, G. Castaldo, A. Bianco, ACE2: the major cell entry receptor for SARS-CoV-2, Lung 198 (2020) 867–877.
[29] Y. Meng, C.-H. Yu, W. Li, T. Li, W. Luo, S. Huang, P.-S. Wu, S.-X. Cai, X. Li, Angiotensin-converting enzyme 2/angiotensin-(1-7)/Mas axis protects against lung fibrosis by inhibiting the MAPK/NF-κB pathway, Am. J. Respir. Cell Mol. Biol. 50 (2014) 723–736.
[30] F. Perrotta, G. Corbi, G. Mazzeo, M. Boccia, L. Aronne, V.D. Agnano, K. Komici, G. Mazzarella, R. Parrella, A. Bianco, COVID - 19 and the elderly : insights into pathogenesis and clinical decision - making, Aging Clin. Exp. Res. (2020).
[31] M. Watanabe, D. Caruso, D. Tuccinardi, R. Risi, M. Zerunian, M. Polici, F. Pucciarelli, M. Tarallo, L. Strigari, S. Manfrini, et al., Visceral fat shows the strongest association with the need of intensive care in patients with COVID-19, Metabolism 111 (2020) 154319.
[32] M.V. Soto-Abraham, J. Soriano-Rosas, A. Díaz-Quiñónez, J. Silva-Pereyra, P. Vazquez-Hernandez, O. Torres-López, A. Roldán, A. Cruz-Gordillo, P. Alonso-Viveros, F. Navarro-Reynoso, Pathological changes associated with the 2009 H1N1 virus, N. Engl. J. Med. 361 (2009) 2001–2003.
[33] J.R. Gill, Z.-M. Sheng, S.F. Ely, D.G. Guinee, M.B. Beasley, J. Suh, C. Deshpande, D.J. Mollura, D.M. Morens, M. Bray, et al., Pulmonary pathologic findings of fatal 2009 pandemic influenza A/H1N1 viral infections, Arch. Pathol. Lab Med. 134 (2010) 235–243.
[34] N. Tang, H. Bai, X. Chen, J. Gong, D. Li, Z. Sun, Anticoagulant treatment is associated with decreased mortality in severe coronavirus disease 2019 patients with coagulopathy, J. Thromb. Haemostasis (2020).